**✕JGR** Journal of Ginseng Research

# Differential Effects of Ginsenoside Metabolites on HERG K⁺ Channel Currents

Sun-Hye Choi[1][#], Tae-Joon Shin[1][#], Sung-Hee Hwang[1][#], Byung-Hwan Lee[1], Jiyeon Kang[1], Hyeon-Joong Kim[1], Jae-Wook Oh[2], Chun Sik Bae[3], Soo-Han Lee[4], and Seung-Yeol Nah[1*]

[1]Ginsentology Research Laboratory and Department of Physiology, College of Veterinary Medicine and Bio/Molecular Informatics Center, Konkuk University, Seoul 143-701, Korea
[2]College of Food Science and Biotechnology of Animal Resources, Konkuk University, Seoul 143-701, Korea
[3]College of Veterinary Medicine, Animal Medical Institute, Chonnam National University, Gwangju 500-757, Korea
[4]Department of Clinical Pharmacology and Therapeutics, University of Ulsan College of Medicine, Seoul 138-736, Korea

The human *ether-a-go-go*-related gene (HERG) cardiac K⁺ channels are one of the representative pharmacological targets for development of drugs against cardiovascular diseases such as arrhythmia. *Panax ginseng* has been known to exhibit cardio-protective effects. In a previous report we demonstrated that ginsenoside $Rg_3$ regulates HERG K⁺ channels by decelerating deactivation. However, little is known about how ginsenoside metabolites regulate HERG K⁺ channel activity. In the present study, we examined the effects of ginsenoside metabolites such as compound K (CK), protopanaxadiol (PPD), and protopanaxatriol (PPT) on HERG K⁺ channel activity by expressing human α subunits in *Xenopus* oocytes. CK induced a large persistent deactivating-tail current ($I_{deactivating-tail}$) and significantly decelerated deactivating current decay in a concentration-dependent manner. The $EC_{50}$ for persistent $I_{deactivating-tail}$ was 16.6±1.3 μM. In contrast to CK, PPT accelerated deactivating-tail current deactivation. PPD itself had no effects on deactivating-tail currents, whereas PPD inhibited ginsenoside $Rg_3$-induced persistent $I_{deactivating-tail}$ and accelerated HERG K⁺ channel deactivation in a concentration-dependent manner. These results indicate that ginsenoside metabolites exhibit differential regulation on $I_{deactivating-tail}$ of HERG K⁺ channel.

**Keywords:** *Panax ginseng*, Ginsenoside metabolites, Human *ether-a-go-go*-related gene K⁺ channel, Human heart

## INTRODUCTION

K⁺ channels play critical roles in a wide variety of physiological processes, including the regulation of neurotransmitter release, neuronal excitability, heart rate, muscle contraction, hormone secretion, epithelial electrolyte transport, cell volume, and cell proliferation [1]. Cardiomyocytes contain two kinds of delayed rectifier K⁺ channels, which are important for cardiac repolarization after cardiac action potential and shorten the action potential duration [2]. Thus, the human *ether-a-go-go*-related gene (HERG, $I_{Kr}$) and KVLQT (KCNQ) ($I_{Ks}$) K⁺ channels are mainly responsible for repolarization of the heart cardiac action potential [3]. The genetic or patho-

logical dysfunctions of HERG or KCNQ K$^+$ channels are one of the primary triggers of cardiac diseases such as arrhythmias. Since arrhythmias are a major cause of sudden cardiac death in the world [2], HERG as well as KCNQ K$^+$ channels are the principal pharmacological targets for development of therapeutic drugs against cardiovascular diseases including arrhythmias.
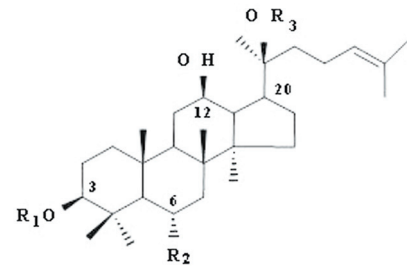
Ginseng, the root of *Panax ginseng* Meyer, has been used as a general tonic to promote longevity and enhance bodily functions against stress, fatigue, diseases, cancer and diabetes mellitus [4]. Among various ginseng components, ginsenosides (also called ginseng saponins) exhibit anti-hypertension and cardio-protective effects [5]. In a previous study, we demonstrated that ginsenoside Rg$_3$ (Rg$_3$) enhanced cardiac $I_{Ks}$ channel currents, which consist of KCNQ1 plus KCNE1 subunits in both concentration- and voltage-dependent manners [6]. In addition, we also demonstrated that Rg$_3$ enhanced outward currents ($I_{HERG}$) and transient tail currents ($I_{tail}$). Rg$_3$ induced a large persistent deactivating-tail current ($I_{deactivataing-tail}$) and significantly decelerated deactivating current decay [7].

On the other hand, ginsenosides administered via the oral route can pass into the large intestine without being broken down by either gastric juices or digestive enzymes [8]. But protopanaxadiol (PPD) ginsenosides are metabolized by intestinal microorganisms into compound K (CK) with one glucose at the C-20 position and are further metabolized to form PPD without glucose, whereas protopanaxatriol (PPT) ginsenosides are metabolized to PPT that only maintains the backbone structure of ginsenosides without any carbohydrate component (Fig. 1). The purpose of this study was to investigate how ginsenoside metabolites affect HERG K$^+$ channel activity. We report here that CK decelerated HERG K$^+$ channel deactivation, whereas PPT accelerated HERG K$^+$ channel deactivation. PPD itself had no effect on HERG K$^+$ channel activity but antagonized Rg$_3$-mediated HERG K$^+$ channel regulations. These results indicate that ginsenoside metabolites exhibit differential regulation on HERG K$^+$ channel activity.

## MATERIALS AND METHODS

### Materials

The individual ginsenoside Rg$_3$ and ginsenoside metabolites such as PPD, PPT, and CK were provided by AMBO Institute (Seoul, Korea) (Fig. 1A). The cDNAs for human HERG K$^+$ channels (accession no. U04270) were kindly provided by Dr. Pongs (University of Ham-



**Fig. 1.** Chemical structures of ginsenoside Rg$_3$ and ginsenoside metabolites used in this study. CK, compound K; PPD, protopanaxadiol; PPT, protopanaxatriol; Glc, glucopyranoside.

| Ginsenosides | R1 | R2 | R3 |
|---|---|---|---|
| CK | -H | -H | -Glc |
| Rg$_3$ | -Glc$_2$-Glc | -H | -H |
| PPD | -H | | -H |
| PPT | -H | -OH | -H |

burg, Germany). All other reagents were purchased from Sigma-Aldrich (St. Louis, MO, USA).

### Preparation of *Xenopus* oocytes and microinjection

*Xenopus laevis* frogs were purchased from *Xenopus* I (Ann Arbor, MI, USA). Their care and handling were in accordance with the highest standards of institutional guidelines of Konkuk University. For isolation of oocytes, frogs were anesthetized with an aerated solution of 3-amino benzoic acid ethyl ester followed by removal of ovarian follicles. The oocytes were treated with collagenase and then agitated for 2 h in Ca$^{2+}$-free medium containing 82.5 mM NaCl, 2 mM KCl, 1 mM MgCl$_2$, 5 mM HEPES, 2.5 mM sodium pyruvate, 100 units/mL penicillin and 100 μg/mL streptomycin. Stage V-VI oocytes were collected and stored in ND96 medium (in mM: 96 NaCl, 2 KCl, 1 MgCl$_2$, 1.8 CaCl$_2$, and 5 HEPES, pH 7.5) supplemented with 50 μg/mL gentamicin. The oocyte-containing solution was maintained at 18°C with continuous gentle shaking and renewed daily. Electrophysiological experiments were performed within 5-6 days of oocyte isolation, with ginsenoside Rg$_3$ or ginsenoside metabolites added to the bath. For HERG K$^+$ channel experiments, HERG K$^+$ channel-encoding cRNAs (40 nL) were injected into the animal or vegetal pole of each oocyte one day after isolation, using a 10 μl microdispenser (VWR Scientific, San Francisco, CA, USA) fitted with a tapered glass pipette tip (15-20 μm in diameter) [9].

## Data recording

A custom-made Plexiglas net chamber was used for two-electrode voltage-clamp recordings as previously reported [7]. The oocytes were impaled with two microelectrodes filled with 3M KCl (0.2-0.7 MΩ), and electrophysiological experiments were carried out at room temperature using an Oocyte Clamp (OC-725C; Warner Instruments, Hamsden, CT, USA). Stimulation and data acquisition were controlled with a pClamp 8 (Axon Instruments, Union City, CA, USA). For most electrophysiological experiments, oocytes were initially perfused with ND96 solution (in mM: 96 NaCl, 3 KCl, 2 CaCl$_2$, 5 HEPES, pH 7.4 with NaOH) to obtain control current recordings. The oocytes were then clamped at a holding potential of −90 mV, the membrane potential was depolarized to 0 mV for 4 s, followed by repolarization to −60 mV at 20 s intervals, and current values were recorded.

## Data analysis

To obtain the concentration-response curve of the respective ginsenoside metabolites effects on the K$^+$ current from the HERG K$^+$ channel, the peak amplitudes at various concentrations of the respective ginsenoside metabolites were plotted, and Origin software (Origin, Northampton, MA, USA) was used to fit the plot to the Hill equation: $y/y_{max} = [A]^{nH}/([A]^{nH} + [IC_{50}]^{nH})$, where y is the peak current at a given concentration of ginsenoside metabolite, $y_{max}$ is the maximal peak current, $EC_{50}$ is the concentration of the respective ginsenoside metabolite producing a half-maximal effect, [A] is the concentration of the respective ginsenoside metabolite, and nH is the Hill coefficient. All values were presented as the mean±SEM. The significance of differences between mean control and treatment values was determined using Student's t-test, where $p < 0.05$ was considered statistically significant.

## RESULTS AND DISCUSSION

### Effects of CK on HERG K$^+$ channel currents

We first examined the effect of intermediate ginsenoside metabolite CK on the HERG K$^+$ channel currents using a *Xenopus* oocyte gene expression system. HERG K$^+$ channel currents were recorded using the two-electrode voltage-clamp recording technique at room temperature [10]. Throughout these experiments, the holding potential was maintained at −90 mV and repolarized to −60 mV after depolarizing pulses from 0 mV, unless otherwise indicated. Fig. 2A gives an example of a voltage-clamp recording with the representative current traces of $I_{HERG}$ at end of depolarization, transient peak $I_{tail}$, and slow $I_{deactivating-tail}$ as indicated by arrows in the absence or presence of various concentrations of CK. CK had almost no effect on $I_{HERG}$ and $I_{tail}$ (Fig. 2A). Interestingly, CK showed a major effect on slow $I_{deactivating-tail}$. Thus in the presence of CK, $I_{deactivating-tail}$ failed to decay, and instead, a large persistent outward current developed. CK (100 μM) increased slow $I_{deactivating-tail}$ by an average of 97.8±8.13% compared to control (Fig. 2A). CK response was completely reversible upon washing the oocytes with ND96 (data not shown). Next, we examined the concentration-dependent effect of CK on $I_{HERG}$, $I_{tail}$, and slow $I_{deactivating-tail}$. As shown in Fig. 2B, CK had a negligible effect on both $I_{HERG}$ and $I_{tail}$. CK also increased a persistent $I_{deactivating-tail}$ in a concentration-dependent manner. The $EC_{50}$ value was16.6±1.3 μM for slow $I_{deactivating-tail}$.

Next, we investigated the HERG K$^+$ current-voltage (I-V) relationship using CK (Fig. 2C, D). The amplitude of $I_{HERG}$ measured at the end of depolarization increased with increasing positive voltage steps, reaching a maximum at −10 mV and then progressively decreased with further voltage steps in the control, indicating that HERG K$^+$ channel is activated with rectified manner (Fig. 2C, D). When the amplitude of $I_{HERG}$ was normalized to the maximum amplitude of the $I_{HERG}$ obtained under the control conditions and was plotted against the potential of the step depolarization (Fig. 2C, D), the presence of various concentrations of CK did not show a significant increase of $I_{HERG}$ even at high concentrations of CK, indicating that CK mainly affects slow $I_{deactivating-tail}$.

We next examined whether CK affects steady-state activation (Fig. 2E). Treatment of 10 and 30 μM CK caused significant leftward shifts in steady-state activation curves compared to control oocytes. The $V_{1/2}$ values were −25.5±0.39 mV in the control and −24.6±0.43, −30.9±0.50 and −32.4±0.82 mV in the presence of 3, 10, and 30 μM CK-treated groups, respectively ($p < 0.05$ at 10 and 30 μM Rg$_3$ compared to control, n=5). The slope factors (kg) were not significantly changed, yielding values of 6.7±0.34 in control and 6.3±0.37, 6.1±0.44 and 6.5±0.70 in the presence of 3, 10 and 30 μM CK-treated groups, respectively. We also examined CK (30 μM) and observed that it did not affect steady-state inactivation (data not shown). Therefore, these results indicate that CK affects the activation gating rather than inactivation gating of HERG K$^+$ channels.

### Effects of PPT on HERG K$^+$ channel currents

PPT had no effects on $I_{HERG}$ and $I_{tail}$ as observed with CK. However, PPT showed a significant effect on slow
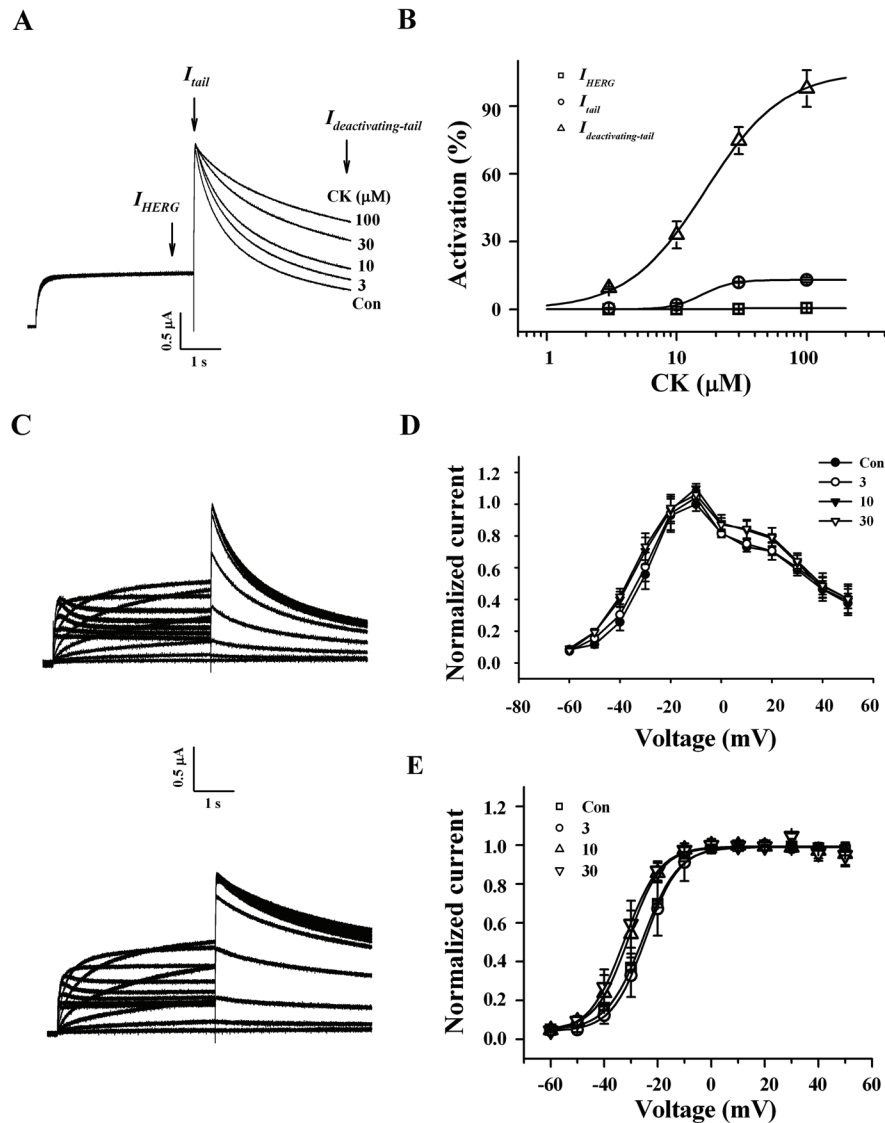
**Fig. 2.** Effects of compound K (CK) on $I_{HERG}$, $I_{tail}$, and $I_{deactivating-tail}$. (A) Representative current traces on human *ether-a-go-go*-related gene (HERG) K+ channel enhancements by various concentrations of CK. Currents were in response to 4-s voltage steps to 0 mV from a holding potential of –90 mV, followed by repolarization to –60 mV. $I_{HERG}$ was obtained at the end of depolarization; $I_{tail}$ was obtained at beginning of repolarization; slow $I_{deactivating-tail}$ was obtained at the end of repolarization as indicated by arrow in (A). (B) Concentration-response curves for the activation of HERG K+ currents by CK on $I_{HERG}$, $I_{tail}$, and $I_{deactivating-tail}$. Solid lines were fitted to the Hill equation. CK was potent for the enhancement of $I_{deactivating-tail}$. Bars represent the means±SEM (*n*=5-7). (C) The representative control (upper traces) and 100 μM CK-mediated currents (down traces) in I-V relationship. Currents were recorded at test potential from –60 to +50 mV. $I_{tail}$ and $I_{deactivating-tail}$ were recorded after repolarization to –60 mV. (D) I-V relationships for HERG K+ currents measurement at the end of the 4-s test pulse before and after application of 3, 10, and 30 μM CK (*n*=5). Currents were normalized to the control current at 0 mV for each oocyte. Data are represented by the means±SEM (*n*=7). (E) Effects of CK on the steady-state activation curve for HERG K+ channel. $I_{tail}$ were normalized to the peak current under each condition, and the data were fitted with a Boltzmann function. Treatment of CK (10, 30, and 100 μM) did cause a leftward shift. Con, control.

$I_{deactivating-tail}$. As a result, in the presence of PPT, $I_{deactivating-tail}$ accelerated to decay in contrast to CK. PPT (100 μM) decreased slow $I_{deactivating-tail}$ by an average of 88.2±1.3% compared to control (Fig. 3A). PPT response was also completely reversible upon washing the oocytes with

ND96 (data not shown). Next, we examined the concentration-dependent effect of PPT on $I_{HERG}$, $I_{tail}$, and slow $I_{deactivating-tail}$. As shown in Fig. 3B, PPT showed a slight inhibition on $I_{tail}$ but a negligible effect on $I_{HERG}$, however PPT primarily inhibited $I_{deactivating-tail}$ in a concentration-
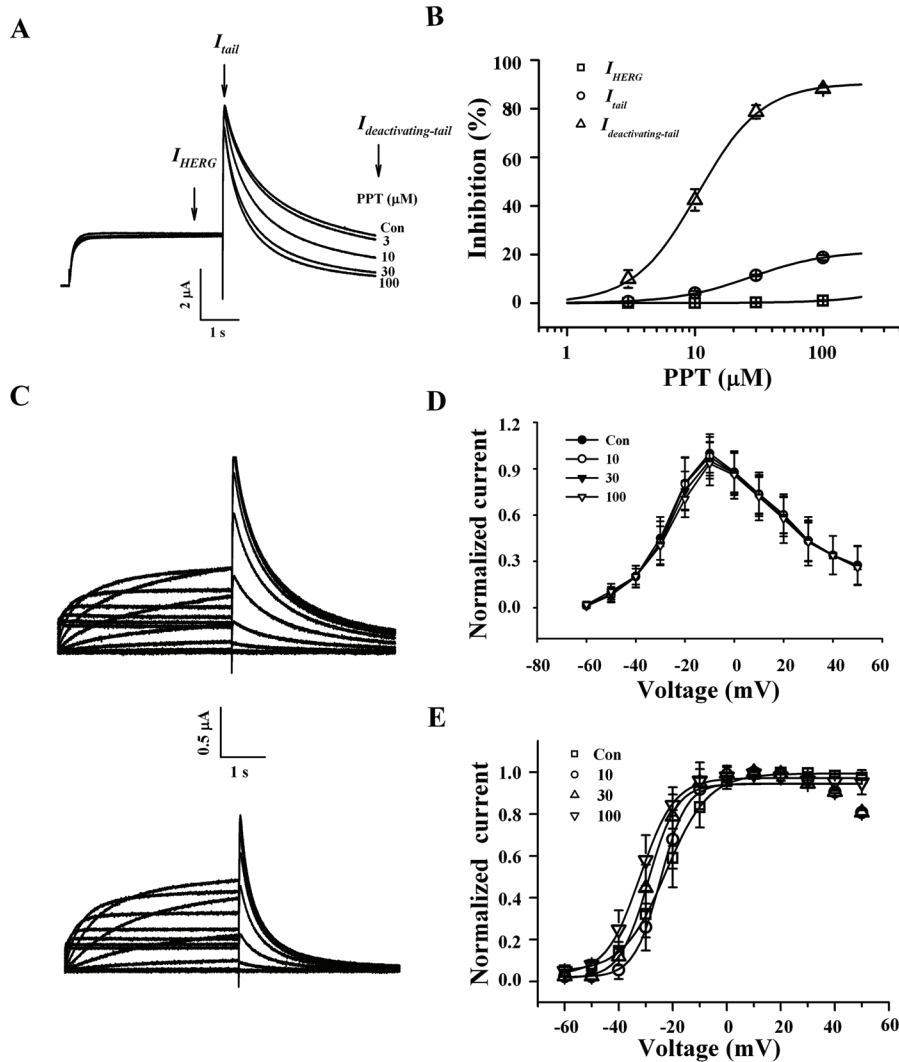
**Fig. 3.** Effects of protopanaxatriol (PPT) on $I_{HERG}$, $I_{tail}$, and $I_{deactivating-tail}$. (A) Representative current traces on human *ether-a-go-go*-related gene (HERG) K⁺ channel inhibitions by various concentrations of PPT. Currents were in response to 4-s voltage steps to 0 mV from a holding potential of –90 mV, followed by repolarization to –60 mV. $I_{HERG}$ was obtained at the end of depolarization; $I_{tail}$ was obtained at beginning of repolarization; slow $I_{deactivating-tail}$ was obtained at the end of repolarization as indicated by the arrow. (B) Concentration-response curves for the inhibition of HERG K⁺ currents by PPT on $I_{HERG}$, $I_{tail}$, and $I_{deactivating-tail}$. Solid lines were fitted to the Hill equation. PPT was potent for the inhibition of $I_{deactivating-tail}$. Bars represent the means±SEM (*n*=5-7). (C) The representative control (upper traces) and 100 μM PPT-mediated currents (down traces) in I-V relationship. Currents were recorded at test potential from –60 to +50 mV. $I_{tail}$ and $I_{deactivating-tail}$ were recorded after repolarization to –60 mV. (D) I-V relationships for HERG K⁺ currents measurement at the end of the 4-s test pulse before and after application of 3, 10, and 30 μM PPT (*n*=5). Currents were normalized to the control current at 0 mV for each oocyte. Data are represented by the means±SEM (*n*=7). (E) Effects of PPT on the steady-state activation curve for HERG K⁺ channel. $I_{tail}$ were normalized to the peak current under each condition, and the data were fitted with a Boltzmann function. Treatment of PPT (3, 10, and 30 μM) did not cause a leftward shift. Con, control.

dependent manner. Interestingly, PPT had a considerable effect on $I_{deactivating-tail}$ compared to $I_{HERG}$ and $I_{tail}$. The $IC_{50}$ value was 27.5±2.3 μM for slow $I_{tail}$, while the $IC_{50}$ value was 10.6±0.5 μM for slow $I_{deactivating-tail}$.

Next, we examined the HERG K⁺ current-voltage (I-V) relationship using PPT (Fig. 3C, D). The amplitude of $I_{HERG}$ measured at the end of depolarization increased with increasing positive voltage steps, reaching a maximum at –10 mV and then progressively decreased with further voltage steps in the control, indicating that HERG K⁺ channel rectifies (Fig. 3C, D). When the amplitude of $I_{HERG}$ was normalized to the maximum amplitude of the $I_{HERG}$ obtained under the control conditions and was plotted against the potential of the step depolarization (Fig.

3C, D), the presence of various concentrations of PPT did not show a significant increase of $I_{HERG}$ even at high concentrations of PPT, indicating that PPT mainly affects slow $I_{deactivating-tail}$.

We next set forth to determine whether PPT affects steady-state activation (Fig. 3E). Treatment of 10 and 30 μM PPT did induce slightly but not significant leftward shifts in steady-state activation curves compared to control oocytes. The $V_{1/2}$ values were –22.6±0.37 mV in the control and –28.7±1.35, –29.1±1.43 and –30.1±0.46 mV in the presence of 3, 10, and 30 μM PPT-treated groups, respectively ($p$<0.08 at 10 and 30 μM Rg$_3$ compared to control, $n$=5). The slope factors ($kg$) were not significantly changed, yielding values of 7.9±0.33 in control and 4.8±0.09, 5.2±1.29 and 6.3±0.39 in the presence of 3, 10 and 30 μM PPT-treated groups, respectively. We also examined PPT (100 μM) and observed that it did not affect steady-state inactivation (data not shown). Therefore, these results indicate that PPT affects the activation gating rather than inactivation gating of HERG K$^+$ channels.

## Effects of PPD on HERG K$^+$ channel currents

PPD itself had nearly no effects on IHERG, $I_{tail}$, and slow $I_{deactivating-tail}$ (Fig. 4A). However, PPD showed an inhibition on Rg$_3$-mediated enhancement on slow $I_{deactivating-tail}$. Hence in the presence of PPD, Rg$_3$-induced persistent $I_{deactivating-tail}$ was greatly attenuated. PPD effect on Rg$_3$-induced persistent $I_{deactivating-tail}$ was completely reversible upon washing the oocytes with ND96 (data not shown). We subsequently examined the concentration-dependent effect of PPD on Rg$_3$-induced persistent $I_{deactivating-tail}$. As shown in Fig. 4B, PPD showed a negligible effect on $I_{HERG}$ and $I_{tail}$ but PPD greatly attenuated Rg$_3$-induced persistent $I_{deactivating-tail}$ in a concentration-dependent manner. Interestingly, PPD caused a rightward shift of Rg$_3$-induced persistent $I_{deactivating-tail}$ from 0.5±0.04 to 2.9±0.57 μM for slow $I_{deactivating-tail}$ (Fig. 4C).

We then studied the HERG K$^+$ current-voltage (I-V) relationship using PPD on Rg$_3$-induced enhancement of $I_{HERG}$ (Fig. 4B). The amplitude of $I_{HERG}$ measured at the end of depolarization increased with increasing positive voltage steps, reaching a maximum at –10 mV and then progressively decreased with further voltage steps in the control, indicating that HERG K$^+$ channel rectifies (Fig. 4B). When the amplitude of $I_{HERG}$ was normalized to the maximum amplitude of the $I_{HERG}$ obtained under the control conditions and was plotted against the potential of the step depolarization (Fig. 4B), the presence of various concentrations of PPD did not show a significant increase of $I_{HERG}$ even at high concentrations of PPD, indicating

that PPD mainly affects Rg$_3$-induced persistent $I_{deactivating-tail}$.

Our following goal was to examine whether PPD affects steady-state activation (Fig. 3E). In contrast to CK or PPT, co-treatment of 10 and 30 μM PPD with Rg$_3$ did not affect on Rg$_3$-caused leftward shifts in steady-state activation curves compared to control oocytes. The $V_{1/2}$ values were –21.7±0.18 mV in the control and –21.2±0.35, –24.6±0.27 and –24.6±0.28 mV in the presence of 3, 10, and 30 μM PPD-treated groups, respectively ($p$<0.07 at 10 and 30 μM Rg$_3$ compared to control, $n$=5). The slope factors ($kg$) were not significantly changed, yielding values of 7.9±0.16 in control and 8.7±0.31, 7.5±0.24 and 7.5±0.25 in the presence of 3, 10 and 30 μM PPD-treated groups, respectively. We also examined PPD (100 μM) and observed that it did not affect steady-state inactivation (data not shown). These results suggest PPD affects the activation gating rather than inactivation gating of HERG K$^+$ channels.

Ginsenosides consist of aglycone and carbohydrates portions. The aglycone is the backbone of the ginsenoside, with a hydrophobic four-ring steroid-like structure that may be non-polar, whereas the carbohydrates on carbons-3, 6, and 20 of the backbone are polar (Fig. 1A). *In vitro* and in *vivo* studies have shown that ginsenosides administered by an oral route were metabolized and finally become an agylcone such as CK which has one glucose at the C-20, PPD and PPT [8]. Recent report showed that these ginsenoside metabolites might also induce apoptosis of the cancer cells and play a role as an anti-cancer agent [8,11], suggesting that ginsenosides are pro-drugs of these metabolites. However, relatively little is known regarding how ginsenoside metabolites regulate ion channel or receptor activity.

In the present study, we report three major findings. First, we observed that CK decelerated deactivating time constants in both concentration- and voltage-dependent manners, whereas CK had no effects on $I_{HERG}$ and $I_{tail}$. Second, we found that PPT accelerated $I_{deactivating-tail}$ deactivation in both concentration- and voltage-dependent manners without affecting on $I_{HERG}$ and $I_{tail}$. Third, PPD itself had no effect on $I_{HERG}$, $I_{tail}$, and $I_{deactivating-tail}$. However, co-treatment of PPD with Rg$_3$ blocked Rg$_3$-mediated decelerating effects on $I_{deactivating-tail}$. Thus, the major findings of the present study are that ginsenoside metabolites had no significant effects on $I_{HERG}$ and $I_{tail}$ of HERG K$^+$ channel but they did affect $I_{deactivating-tail}$ in differing manners, indicating that ginsenoside metabolites show a differential regulation of $I_{deactivating-tail}$ with respect to the HERG K$^+$ channel.
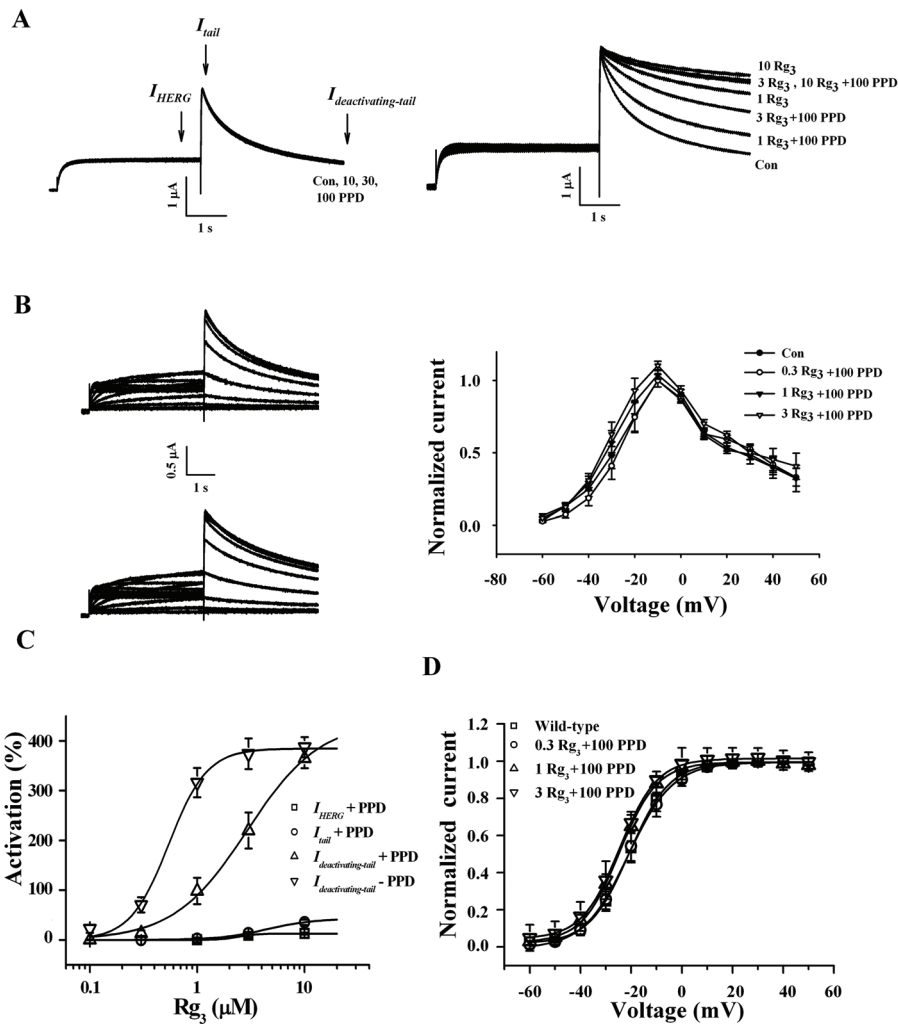
On the other hand, we demonstrated in previous stud-

**Fig. 4.** Effects of protopanaxadiol (PPD) on Rg$_3$-mediated $I_{HERG}$, $I_{tail}$, and $I_{deactivating-tail}$. (A) Representative current traces on human *ether-a-go-go*-related gene (HERG) K$^+$ channel inhibitions by various concentrations of PPD itself (left panel). Currents were in response to 4-s voltage steps to 0 mV from a holding potential of –90 mV, followed by repolarization to –60 mV. $I_{HERG}$ was obtained at the end of depolarization; $I_{tail}$ was obtained at beginning of repolarization; slow $I_{deactivating-tail}$ was obtained at the end of repolarization as indicated by the arrow. Concentration-dependent inhibitions of HERG K$^+$ currents by PPD on Rg$_3$-mediated $I_{HERG}$, $I_{tail}$, and $I_{deactivating-tail}$ (right panel). (B) I-V relationships for HERG K$^+$ currents measurement at the end of the 4-s test pulse before (upper traces) and after application of 1 μM Rg$_3$ plus 100 μM PPD (down traces). Currents were normalized to the control current at 0 mV for each oocyte (right panel). Data are represented by the means±SEM (*n*=7). (C) Concentration-response curves for the activation of HERG K$^+$ currents by Rg$_3$ in the absence or presence of PPD on $I_{HERG}$, $I_{tail}$, and $I_{deactivating-tail}$. Solid lines were fitted to the Hill equation. PPD significantly affected $I_{deactivating-tail}$. Bars represent the means±SEM (*n*=5-7). (D) Effects of PPD on Rg$_3$-mediated the steady-state activation curve for HERG K$^+$ channel. $I_{tail}$ were normalized to the peak current under each condition, and the data were fitted with a Boltzmann function. Treatment of 100 μM PPD in the presence of 0.3, 1, or 3 μM Rg$_3$ did not cause a leftward shift. Con, control.

ies that ginsenoside metabolites such as CK, PPD and PPT regulate ion channels and receptors. For example, CK but not PPT caused strong inhibition of the voltage-dependent α1G-type Ca$^{2+}$ channel [12]. Similarly, we have also found that CK but not M4 (PPT) inhibited a neuronal Na$^+$ (Nav1.2) channel [13]. We demonstrated that M4, but not CK, exhibited an inhibitory effect on 5-HT$_{3A}$ receptor-mediated currents [14]. In addition, CK and PPT exhibited an inhibitory effect on α3β4 nicotinic acetylcholine receptor-mediated currents [15]. All these findings indicate that ginsenoside metabolites as well as ginsenosides have regulatory effects on voltage-dependent ion channel and receptor activities.

Since the HERG K$^+$ channel regulators are clinically important for treatment of cardiac diseases such as arrhythmia, there are numerous reports on the development

of HERG $K^+$ channel regulators from natural compounds [16]. In the previous study, we found that $Rg_3$ increased $I_{HERG}$ and peak $I_{tail}$. In addition, $Rg_3$ profoundly delayed deactivation kinetics by inducing a persistent $I_{deactivating-tail}$ and caused a leftward shift of steady-state voltage-dependent activation but not inactivation, leading to the possibility that $Rg_3$ is an activator to open HERG $K^+$ channel at a more negative voltage step than control and that $Rg_3$ mainly works by slowing closure of the HERG $K^+$ channel once it has opened. In the present study, when we examined the effects of ginsenoside metabolites on HERG $K^+$ channel currents, we found that CK induced a persistent $I_{deactivating-tail}$ and caused a leftward shift of steady-state voltage-dependent activation (Fig. 2). However, the effective concentration of CK was higher than that of $Rg_3$. In contrast to CK, PPT caused an acceleration of $I_{deactivating-tail}$ decay (Fig. 3). Interestingly, co-treatment of PPD with $Rg_3$ blocked $Rg_3$-mediated deceleration of deactivation process. It is noteworthy that since $Rg_3$ became PPD after metabolic process, PPD-mediated antagonism of $Rg_3$ action on HERG $K^+$ channel activity show the possibility that aglycone, PPD, ginsenoside $Rg_3$ and other PPD ginsenosides might interfere with *in vivo* $Rg_3$ actions on HERG $K^+$ channel activity.

Taken together, we found that CK decelerated the deactivation process by inducing a persistent $I_{deactivating-tail}$ with delayed deactivation in HERG $K^+$ channel without affecting $I_{HERG}$ and $I_{tail}$. In contrast, PPT accelerated the deactivation process by inducing an inhibition of $I_{deactivating-tail}$ without affecting $I_{HERG}$ and $I_{tail}$. PPD itself had no observable effects on $I_{HERG}$, $I_{tail}$, and $I_{deactivating-tail}$ but co-treatment of PPD with $Rg_3$ blocked $Rg_3$-mediated a persistent $I_{deactivating-tail}$ with delayed deactivation in HERG $K^+$ channel. These novel findings provide an insight into the molecular action of ginsenoside metabolites on HERG $K^+$ channel activity.

## ACKNOWLEDGEMENTS

## REFERENCES

1. Hille B. Ion channels of excitable membranes. Sunderland: Sinauer Associates, 2001.

2. Robbins J. KCNQ potassium channels: physiology, pathophysiology, and pharmacology. Pharmacol Ther 2001;90:1-19.

3. Tristani-Firouzi M, Sanguinetti MC. Structural determinants and biophysical properties of HERG and KCNQ1 channel gating. J Mol Cell Cardiol 2003;35:27-35.

4. Nah SY. Ginseng, recent advances and trends. Korean J Ginseng Sci 1997;21:1-12.

5. Attele AS, Wu JA, Yuan CS. Ginseng pharmacology: multiple constituents and multiple actions. Biochem Pharmacol 1999;58:1685-1693.

6. Choi SH, Shin TJ, Lee BH, Chu DH, Choe H, Pyo MK, Hwang SH, Kim BR, Lee SM, Lee JH, et al. Ginsenoside Rg3 activates human KCNQ1 K+ channel currents through interacting with the K318 and V319 residues: a role of KCNE1 subunit. Eur J Pharmacol 2010;637:138-147.

7. Choi SH, Shin TJ, Lee BH, Hwang SH, Lee SM, Lee BC, Park CS, Nah SY. Ginsenoside Rg3 decelerates HERG K+ channel deactivation through Ser631 residue interaction. Eur J Pharmacol 2011; Epub ahead of print.

8. Hasegawa H, Suzuki R, Nagaoka T, Tezuka Y, Kadota S, Saiki I. Prevention of growth and metastasis of murine melanoma through enhanced natural-killer cytotoxicity by fatty acid-conjugate of protopanaxatriol. Biol Pharm Bull 2002;25:861-866.

9. Lee JH, Lee BH, Choi SH, Yoon IS, Pyo MK, Shin TJ, Choi WS, Lim Y, Rhim H, Won KH, et al. Ginsenoside Rg3 inhibits human Kv1.4 channel currents by interacting with the Lys531 residue. Mol Pharmacol 2008;73:619-626.

10. Sanguinetti MC, Jiang C, Curran ME, Keating MT. A mechanistic link between an inherited and an acquired cardiac arrhythmia: HERG encodes the IKr potassium channel. Cell 1995;81:299-307.

11. Wakabayashi C, Murakami K, Hasegawa H, Murata J, Saiki I. An intestinal bacterial metabolite of ginseng protopanaxadiol saponins has the ability to induce apoptosis in tumor cells. Biochem Biophys Res Commun 1998;246:725-730.

12. Lee JH, Jeong SM, Kim JH, Lee BH, Yoon IS, Lee JH, Choi SH, Lee SM, Park YS, Lee JH, et al. Effects of ginsenosides and their metabolites on voltage-dependent Ca(2+) channel subtypes. Mol Cells 2006;21:52-62.

13. Kim JH, Hong YH, Lee JH, Kim DH, Nam G, Jeong SM, Lee BH, Lee SM, Nah SY. A role for the carbohydrate portion of ginsenoside Rg3 in Na+ channel inhibition. Mol Cells 2005;19:137-142.

14. Lee BH, Jeong SM, Lee JH, Kim DH, Kim JH, Kim JI, Shin HC, Lee SM, Nah SY. Differential effect of ginsen-

oside metabolites on the 5-HT3A receptor-mediated ion current in Xenopus oocytes. Mol Cells 2004;17:51-56.

15. Lee JH, Jeong SM, Lee BH, Kim DH, Kim JH, Kim JI, Lee SM, Nah SY. Differential effect of bovine serum albumin on ginsenoside metabolite-induced inhibition of alpha3beta4 nicotinic acetylcholine receptor expressed in Xenopus oocytes. Arch Pharm Res 2003;26:868-873.

16. Scholz EP, Zitron E, Kiesecker C, Luck S, Thomas D, Kathofer S, Kreye VA, Katus HA, Kiehn J, Schoels W *et al*. Inhibition of cardiac HERG channels by grapefruit flavonoid naringenin: implications for the influence of dietary compounds on cardiac repolarisation. Naunyn Schmiedebergs Arch Pharmacol 2005;371:516-525.